11-25-2011

Scalable nano-patterning of graphenes using laser shock

Li J.
Purdue University

R. J. Zhang
Purdue University, zhang169@purdue.edu

H. Q. Jiang

G. J. Cheng

Follow this and additional works at: http://docs.lib.purdue.edu/nanopub

Part of the Nanoscience and Nanotechnology Commons

J., Li; Zhang, R. J.; Jiang, H. Q.; and Cheng, G. J., "Scalable nano-patterning of graphenes using laser shock" (2011). *Birck and NCN Publications*. Paper 833.
http://dx.doi.org/10.1088/0957-4484/22/47/475303

Scalable nano-patterning of graphenes using laser shock

J Li[1,4]**, R J Zhang**[2,3,4]**, H Q Jiang**[3] **and G J Cheng**[1]

[1] Birck Nanotechnology Center and School of Industrial Engineering, Purdue University,
West Lafayette, IN 47907, USA
[2] Department of Physics, Wuhan University, Wuhan, 430072, People's Republic of China
[3] School for Engineering of Matter, Transport and Energy, Arizona State University, Tempe,
AZ 85287, USA

E-mail: hanqing.jiang@asu.edu and gjcheng@purdue.edu

Abstract
Nano-patterning of graphene film by a novel approach making use of laser ablation generated pressure is presented in this paper. Arrays of nanoscale holes were fabricated by applying laser shock pressure on graphene film suspended on well trenches in silicon substrate. Round holes with diameters ranging from 50 to 200 nm on graphene film were successfully punched. The critical pressure was found to be dependent on the diameter of holes. The smaller the diameters, the higher the critical pressure, which was also captured by the molecular dynamic (MD) simulations. The laser shock based approach presented in this paper provides an effective way to pattern graphene film with nanoscale features in an easy, fast, and scalable manner.

S Online supplementary data available from stacks.iop.org/Nano/22/475303/mmedia

(Some figures may appear in colour only in the online journal)

1. Introduction

Graphene, a two-dimensional material with covalently bonded carbon atoms packed in a honeycomb lattice, has attracted a great deal of attention due to its unique properties, including structural perfection, low density, excellent electrical properties (e.g. high carrier mobility and saturation velocity [1, 2], zero effective mass near the Dirac point [3], and long mean free path [4]), as well as remarkable mechanical properties [5]. There has been extensive research on the mechanical properties of graphenes. Many experiments have been conducted to determine the Young's modulus and strength using various methods, for example, using atomic force microscopy (AFM) to measure the effective spring constants of graphene and extract the Young's modulus to be 0.5 TPa [6], using nano-indentation with AFM to obtain the Young's modulus of 1.0 TPa, breaking strength of 42 N m^{-1} and intrinsic stress of 130 GPa [7]. In addition to experimental studies, atomistic simulations have also been utilized to study the mechanical properties of graphenes and their findings agree qualitatively with the experimental measurement, such as by

using the *ab initio* method, the Young's modulus is calculated to be 1.05 TPa, and the ultimate tensile strength is 110–121 GPa [8], and by molecular dynamics (MD) methods the Young's modulus is found to vary from 0.95 to 1.1 TPa as temperature increases from 100 to 500 K [9].

These remarkable properties make graphene a promising material for future microscale and nanoscale electronics, optoelectronics, mechanics, and as an alternative platform to silicon based mesostructures. Many of these potential applications, such as high speed field effect transistors, need to open up the bandgap for graphenes since at room temperature graphene is a semimetal with a zero bandgap [3, 10]. Researchers have been using different methods to open up the bandgap for graphenes. Among the methods being developed to open up the bandgap, patterning of graphenes is a promising one. Lithography based methods have been used, such as patterned graphene electrodes from photolithography [11], graphene nanodisk arrays from nanosphere lithography [12], graphene quantum dots from electron beam (e-beam) lithography [13], multilayered graphene nanoribbons from focused ion beam (FIB) lithography [14], and graphene nanomeshes by block copolymer lithography [15] and by nanoimprint lithography [16]. Transfer printing [17, 18] and

---
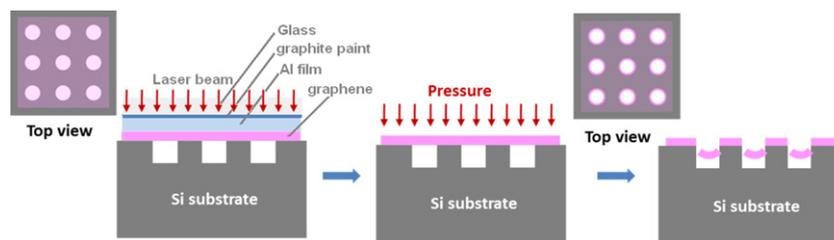
[4] Both authors contribute equally.

Figure 1. Illustration of the laser shock patterning of graphene.

the direct-write process [19–22] are also used. However, these processes are not scalable due to the high expense and slow serial process. For example, direct-write etching with an e-beam in a transmission electron microscope (TEM) relies on transferring graphene flakes onto TEM grids, which are not suitable for larger-scale fabrication of devices [19]; helium ion microscopy replies on high-resolution imaging technology but there are challenges regarding large-scale fabrication [20–22].

We here report a fast and effective approach for the nanoscale punching and patterning of graphene film by making use of laser ablation generated shock pressure. Arrays of holes with diameters of 50, 100 and 200 nm were successfully patterned on single layer graphene films, which were observed by scanning electron microscopy (SEM) and AFM. It is found that a laser shock pressure of 1.9 GPa is needed to successfully punch through the ultrastrong single layer carbon atoms to generate a hole 50 nm in diameter, and the pressure value decreases to pattern larger features because of the size effect. MD simulation and numerical estimation were carried out to study the dynamic punching process of graphene and the relationship between the applied pressure and the dimensions of the holes. The calculated results are in good agreement with the experiments.

2. Results and discussion

The patterning of graphene film is accomplished by a strong and short laser shock impact. As a pulsed laser beam (5 ns, 1064 nm) transmits the SiO_2 glass and radiates an ablative coating (graphite paint), a strong plasma zone is generated and confined by the glass. This confinement results in large shock pressure, which is applied onto the aluminum thin film ($\sim$1 μm) and graphene. The aluminum thin film is used to transform the nanoscale shaping onto the graphene and also to protect the graphene from being ablated by the laser. The duration of the impact is only tens of nanoseconds, and the peak pressure value is about 1–2 GPa. The chemical vapor deposition (CVD) grown graphene film is originally lying over a patterned silicon mold fabricated from FIB milling. During the shock, the graphene film that is suspended on the well positions is suddenly pushed into the cavities and finally pulled off at the edges, leaving patterns of corresponding shapes on the graphene film. After the strong impact, the graphene film is punched through at the well positions and arrays of round holes are patterned on the film. The whole patterning process is completed in a one-step operation and within tens of nanoseconds, which is illustrated in figure 1.

Figure 2(a) shows the typical SEM image of the graphene film lying over a Si substrate patterned with circular wells. The diameter of the wells is 100 nm and the depth is 80 nm. The graphene film is confirmed as single layer with good quality by Raman spectroscopy (figure S1 available at stacks. iop.org/Nano/22/475303/mmedia). The parts of graphene film suspended on the well positions can be seen as free-standing membranes. As the CVD grown graphene film is transferred by a PMMA (polymethyl methacrylate) assisted process, there are some PMMA residuals left on the surface of the graphene. During the laser shock experiment, the free-standing membranes on the well openings are hit by the shock pressure. The pressure is gradually increased each time by increasing the laser intensity, until the membrane is punched through along the well edges. As a result, arrays of round holes are patterned on the graphene film, as illustrated by figures 2(b) and (c). As seen in figure 2(c), some of the broken pieces of graphene are left on the sample after the shock operation. The round shape of the broken piece with a radius of about 50 nm indicates the well punching quality of the membrane across the mold cavity, leaving fairly neat and sharp breaking edges on the patterned graphene.

Morphologies of the graphene film before and after laser shock operation are shown in figures 2(d)–(f). As given by figure 2(d), the graphene film suspended on nanocircular wells is very flat, with an overall roughness of about 3 nm, which is caused by both the PMMA residuals and also the slight pre-tension of graphene film across the well openings [7]. The pre-tension of graphene membranes across openings is due to the van der Waals attraction of the membrane to the substrate, which normally results in pre-tension in the membrane. However, as the size of the circular well is very small in our experiment (less than 100 nm in diameter), the resultant stretching of the membrane is very small, which is hardly distinguished from the height profile along the green line in figure 2(d). Figures 2(e) and (f) show the two-dimensional and three-dimensional AFM images of the patterned graphene film after laser shock, further illustrating the effective nano-punching approach by laser shock pressure. The laser shock pressure needed to accomplish this patterning is estimated using Fabbro's model, in which the magnitude of laser shock pressure is dependent on laser intensity, shock impedance of the confining media and ablative coating, and the absorption coefficient of laser energy in plasma generation [23]. A laser intensity of 0.43 GW cm^{-2} is used, which generates a laser shock pressure of about 1.4 GPa according to Fabbro's model. Smaller holes, e.g. 50 nm in diameter, and larger
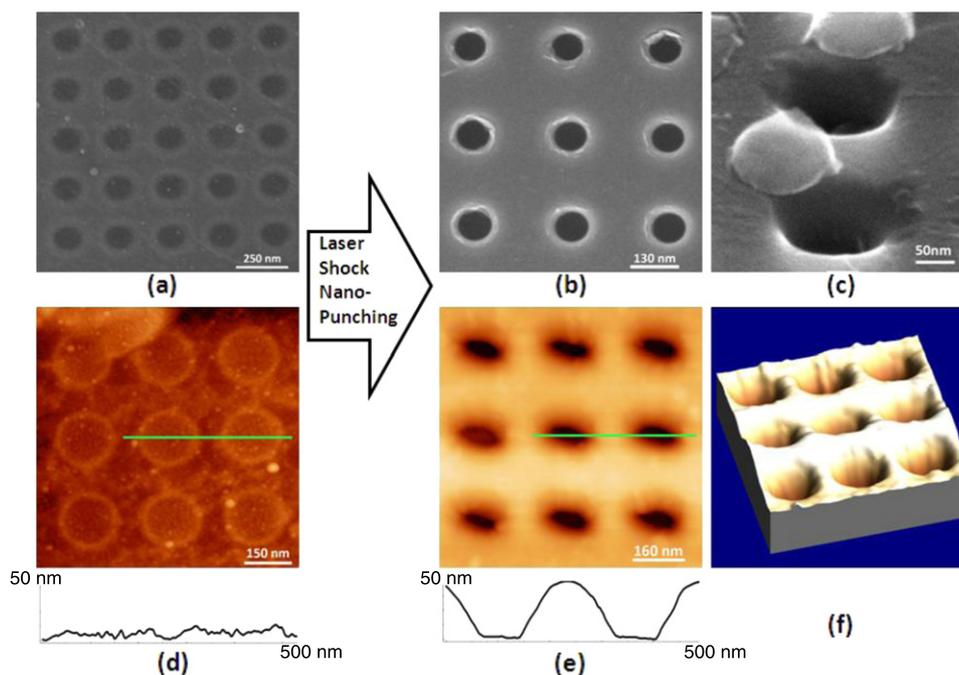
Figure 2. Typical images of patterning graphene film on silicon mold into arrays of circular holes 100 nm in diameter. (a) SEM image of graphene film transferred to a silicon mold patterned with circular wells. (b), (c) SEM images of patterned graphene film after laser shock impact. The film is punched through at the well openings, leaving arrays of round holes on the graphene film. (d) AFM image of graphene film transferred to the silicon mold. (e), (f) Two-dimensional (2D) and three-dimensional (3D) AFM images of graphene film after laser shock impact, with round holes patterned on it. The film is still lying on the Si mold.

holes, e.g. 200 nm in diameter were also successfully punched on graphene films as shown in figure 3. However, features smaller than 50 nm are not patterned in this work due to the difficulty of mold fabrication, but the laser shock approach is still potentially applicable on such a small scale. It is found that with the decreasing of the hole dimension, the difficulty of punching it through increases, indicating a size effect for patterning nano-features. The laser intensity and resultant shock pressure to achieve 50 nm holes are about 0.7 GW cm^{-2} and 1.9 GPa, respectively, and to achieve 200 nm holes are only 0.3 GW cm^{-2} and 1.2 GPa. The size effect is obvious at a size scale less than 100 nm, and should gradually diminish if the feature dimension is further increased.

MD simulations were implemented using LAMMPS [24] to study the nano-patterning process on graphene film. Here, we performed patterning processes of graphene with various hole diameters, ranging from 100 nm, 50 nm, 20 nm, and 10 nm to 5 nm and half-neck-width of 20 nm, 10 nm, 4 nm, 2 nm, and 1 nm, respectively. Figure 4(a) shows a model of one MD simulation of patterning a hole 100 nm in diameter. Among the 746 528 atoms shown in figure 4(a), the gray area represents the carbon atoms suspending on the Si well which are able to move freely (referred to as hole atoms) and the cyan atoms denote carbon atoms on Si mold which are constrained against motion in the perpendicular direction but free to move along the in-plane direction of the graphene (referred to as in-plane atoms). Figure 4(b) shows a representative image of a patterned hole 100 nm in diameter, in which the gray atoms are detached from the graphene. Movies 1 and 2 (available at stacks.iop.org/Nano/22/475303/mmedia) further illustrate

animations showing the dynamic process of patterning a hole 20 nm in diameter in a graphene from different angles.

The critical breaking force for patterning a graphene with holes 100 nm in diameter was simulated to be 0.046 nN for each atom and the corresponding pressure is 1.77 GPa. This calculated pressure agrees with our experiments for the same diameters (1.4 GPa for 100 nm in diameter holes). The slightly larger breaking pressure given by MD simulations can be understood for the following three reasons. (1) The temperature applied in the MD simulation is 300 K while the temperature in the experiment is slightly over 300 K due to the heat generated by the high strain rate deformation in the aluminum film and graphene. The magnitude of this rise is about 50–100 °C depending on the strain rate and the material's thermal properties [25]. Please note that laser heating is not directly absorbed by the aluminum foil but by the graphite coating. (2) The radiation pressure in experiments may also be underestimated due to the underestimation of the reflectivity of graphene. (3) Pre-stretching in the graphene film is induced by the wet transfer process. To evaluate the effect of temperature in patterning the graphene, series studies were conducted to pattern graphenes by varying temperature. Here 20 nm holes were used to save computational cost. Figure 5 shows that the critical breaking pressure decreases significantly with the increase of temperature. The dependence is more sensitive at low temperature. This trend is consistent with the dependence of fracture strength on temperature [26]. The results shown in figure 5 imply that the agreement between the MD simulation and our experiments for patterning holes 100 nm in diameter is actually more convincing as the temperature in experiments is higher, thus the critical breaking pressure decreases.
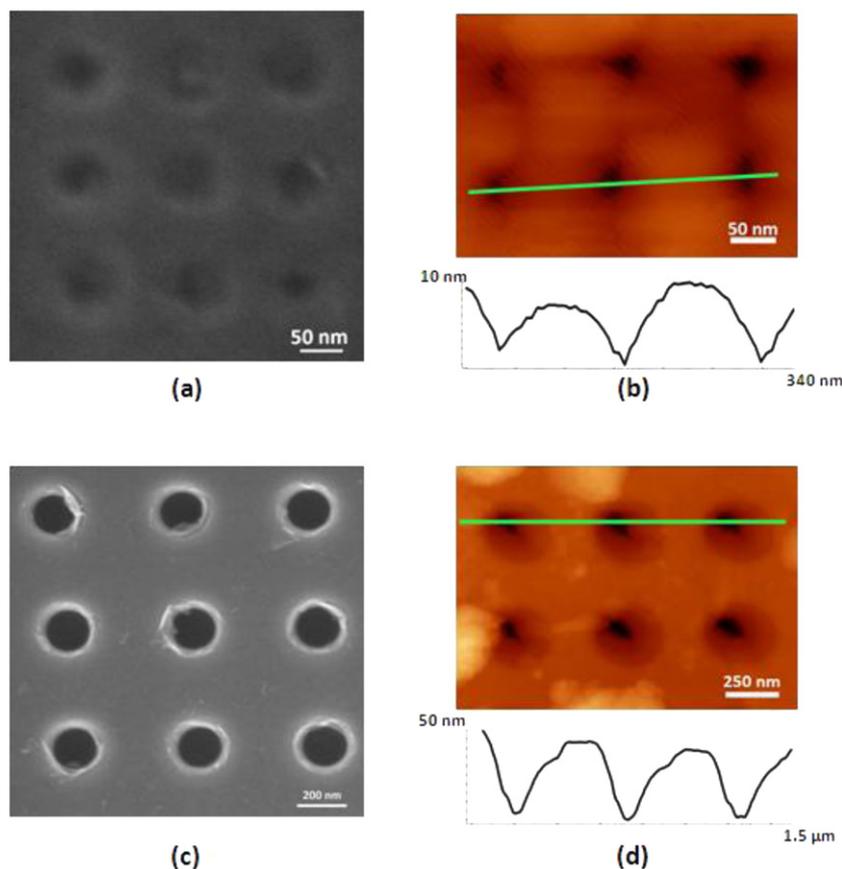
Figure 3. SEM and AFM images of patterned graphene films on a silicon mold with arrays of circular holes with 50 nm ((a) and (b)) and 200 nm ((c) and (d)) diameters.

The effect of hole diameter on the critical breaking pressure was also studied and the results are shown in figure 6(a). It is found that the critical breaking pressure increases dramatically as the diameter of the hole decreases and the relation roughly follows a $1/d$ trend, in which d is the hole diameter. This can be briefly understood as follows. Critical breaking pressure is calculated as Nf/S, in which N is the total number of hole atoms, f is the critical breaking force and also the force applied to each atom and $S = \pi d^2/4$ is the area of the hole. Thus Nf represents the total force applied on the hole atoms. It is suggested that in order to pattern a hole with diameter d, a certain number of carbon bonds that connect the hole atoms and in-plane atoms must be broken and the number of broken bonds is proportional to the hole diameter d, which gives Nf a rough hole diameter d dependence. Thus, the critical break pressure has a $1/d$ dependence, as shown in figure 6(a). Furthermore, it is understood that the number of hole atoms N is proportional to the hole area S as the number density of carbon atoms in a graphene is fairly constant. Given that Nf is proportional to the hole diameter d, the critical breaking force also has a $1/d$ dependence, as shown in figure 6(b).

The leftmost point in figure 6(a) represents an extreme case in which only one honeycomb is to be patterned (figure S2 available at stacks.iop.org/Nano/22/475303/mmedia) and the fracture strength is calculated to be 44.3 N m^{-1} with

corresponding critical breaking pressure 386 GPa. This case is comparable to the uniaxial tension case of graphene in the armchair direction [27], in which the fracture strength was calculated to be 30.2 N m^{-1}. Higher fracture strength for the current case may result for various reasons, such as the higher density of bonds in the present case (i.e. shortened distance between broken bonds) compared with that in uniaxial tension (figure 1 in [27]), and the bond force for bending being a higher order term than tension. In addition to the fracture strength, the 'nominal' fracture strength was also calculated to be 90 GPa by taking the thickness of a graphene as 0.335 nm [27]. One can find that although fracture strength is comparable (44.3 N m^{-1} for patterning versus 30.2 N m^{-1} for uniaxial tension), the 'nominal' fracture strength in uniaxial tension is much less than that in the present simulation. The reason may be the arbitrariness of taking 0.335 nm as the graphene thickness.

3. Conclusion

In summary, we have demonstrated the patterning of nanoscale features on graphene film, by exerting laser shock generated pressure. Arrays of holes 50, 100, and 200 nm diameter were successfully punched. The process is fast, efficient, and scalable. MD simulation was also carried out to study the dynamic punching process. A pressure of 1.77 GPa is calculated to be enough for punching a 100 nm hole, which is
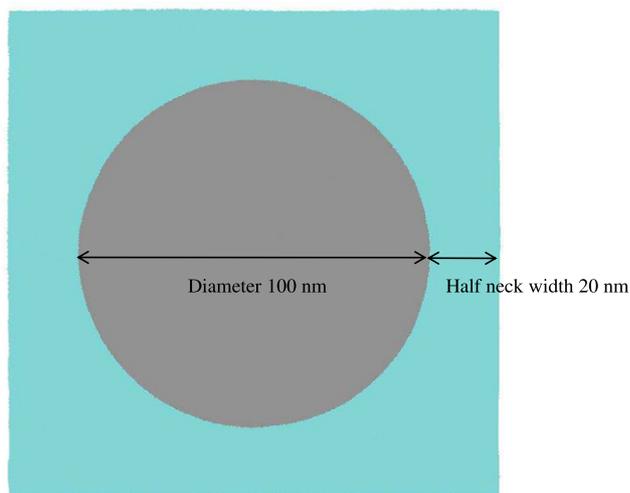
(a)
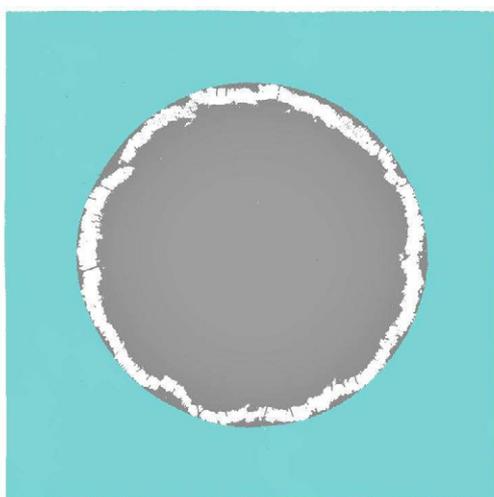
(b)

Figure 4. (a) Initial image of the graphene model in the MD simulation for patterning a hole 100 nm in diameter (hole atoms are represented to be gray); (b) a representative image of a patterned hole 100 nm in diameter.

in good agreement with the critical pressure value of 1.4 GPa in experiment. The smaller the hole is, the higher the critical breaking pressure is. The relation between the applied pressure and the dimension of the hole roughly follows a $1/d$ trend. The presented effective approach to nano-pattern graphene film in a scalable way has great potential to be applied in graphene property adjustment and graphene device fabrication.

4. Experimental section

4.1. Preparation of graphene film

Monolayer graphene was grown by CVD (CH_4 as carbon stock) on Cu foils (25 μm thick, Alfa Aesar, 99.8%) at ambient pressure. The Cu foil was loaded into a CVD furnace and heated to 1050 °C in 300 sccm of flowing Ar and 10 sccm of flowing H_2. After 1050 °C was attained, the sample was
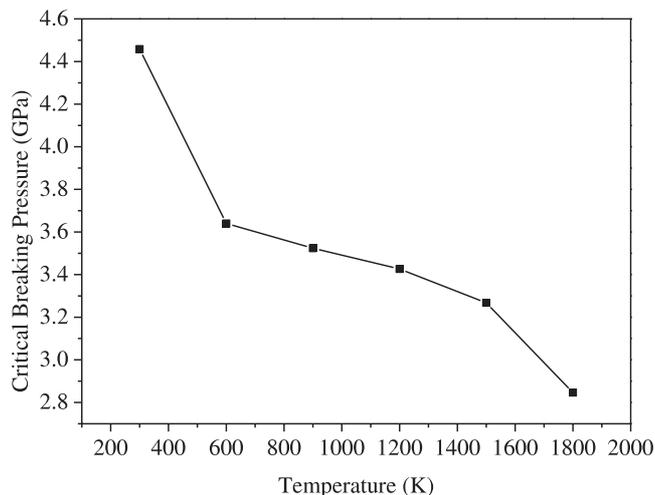
Figure 5. Dependence of critical breaking pressure on the temperature of patterning a hole 20 nm in diameter in graphene.

annealed for at least 30 min without changing the gas flow rates. Then CH_4 (concentration 8 ppm) was injected into the furnace at 300 sccm for 10 min before the system was cooled to room temperature under protection of Ar and H_2. After the growth process, the graphene samples were transferred by a PMMA (polymethyl methacrylate) assisted process in a Cu etchant (iron nitrate) onto Si wafer with arrays of nanoscale circular wells.

4.2. Preparation of silicon mold

Focused ion beam (FIB) milling was used to cut patterns on silicon wafers. The FIB milling was performed by FEI Nova 200 Nano-Lab DualBeam TM-SEM/FIB.

4.3. Setup of the laser shock process

The laser shock process is similar to the one used in laser dynamic forming of thin films [28]. The setup includes a laser source, a transparent confinement, a layer of ablative coating, and a ultrathin metal foil. A short pulsed *Q*-switch Nd-YAG (Continuum® Surelite III) is used as the energy source. The laser beam has a Gaussian distribution and the pulse width is 10 ns. A focus lens is used to control the beam size. The beam diameter used is 4 mm, which is calibrated by a photosensitive paper (Kodak Linagraph, type: 1895). A glass slide was used as the confining media, and aerosol graphite painting (Asbury Carbons, USA) was sprayed on 4 μm thick aluminum foil (Lebow Company Inc, Bellevue, WA) as the ablative coating. The thickness of the ablative coating is in the range from 1 to 10 μm. An *X*–*Y* stage is used to move the processing stage.

4.4. Characterization methods

Raman spectroscopy was performed using a HORIBA Jobin Yvon XploRA confocal Raman microscope equipped with a motorized sample stage from Märzhäuser Wetzlar (00-24-427-0000). The wavelength of the excitation laser was 532 nm and the power of the laser was kept below 2 mW without noticeable

(a)

(b)
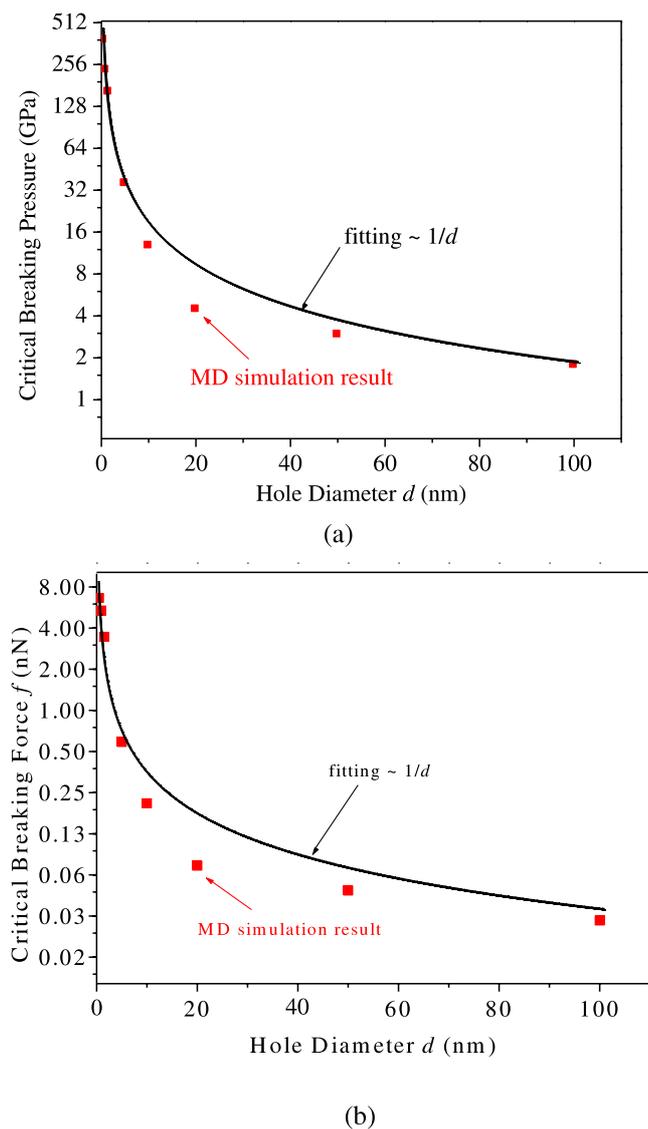
Figure 6. (a) Dependence of critical breaking pressure on hole diameter. (b) Dependence of critical breaking force on hole diameter.

sample heating. The laser spot size was ∼0.6 μm with a 100× objective lens. The SEM image was recorded on a Hitachi S-4800 field-emission scanning electron microscope or a FEI Nova 200 Nano-Lab DualBeam TM-SEM/FIB. The AFM images and height profile were measured by a DI Dimension 3100 atomic force microscope.

4.5. Molecular dynamic (MD) simulations

MD simulations were implemented using LAMMPS [24] to study the nano-patterning process on graphene film. The adaptive intermolecular reactive empirical bond order (AIREBO) potential was used and the cutoff parameter is set to 2.0 Å [24, 29] in order to avoid the spuriously high bond forces and nonphysical results near the fracture region. The periodic boundary condition was used to reproduce the arrays of holes in the MD simulations. Starting with a uniformly distributed initial velocity profile, an isothermal–isobaric (*NPT*) ensemble was implemented for 50 ps with a time step of 0.5 fs to allow

the system reach its equilibrium configuration [26]. Then a prescribed loading force vertical to the graphene film was added to the hole atoms (gray ones in figure 3(a)) to simulate the patterning process. In this process, the *NVE* ensemble was used with a time step of 0.1 fs [30]. This time step ensures convergence after comparing it with a time step of 0.005 fs. The following method was implemented to determine the critical breaking force of graphene with specified holes of different diameters. For two loading forces F_a and F_b, if F_a is able to pattern a hole and F_b is not and the difference between these two loading forces is smaller than a very small criterion, such as 0.005 eV Å^{-1} (0.008 nN) used in the current study, then the average of F_a and F_b is used as the critical breaking force of this system. The corresponding critical breaking pressure is then calculated based on the total critical breaking force applied on all the carbon atoms that are suspended on the Si well divided by the area of the hole.

References

[1] Geim A K and Novoselov K S 2007 The rise of graphene *Nature Mater.* **6** 183–91
[2] Heersche H B, Jarillo-Herrero P, Oostinga J B, Vandersypen L M K and Morpurgo A F 2007 Bipolar supercurrent in graphene *Nature* **446** 56–9
[3] Novoselov K S, Geim A K, Morozov S V, Jiang D, Katsnelson M I, Grigorieva I V, Dubonos S V and Firsov A A 2005 Two-dimensional gas of massless Dirac fermions in graphene *Nature* **438** 197–200
[4] Gunlycke D, Lawler H M and White C T 2007 Room-temperature ballistic transport in narrow graphene strips *Phys. Rev.* B **75** 5
[5] Zhao Q, Nardelli M B and Bernholc J 2002 Ultimate strength of carbon nanotubes: a theoretical study *Phys. Rev.* B **65** 144105
[6] Frank I W, Tanenbaum D M, Van der Zande A M and McEuen P L 2007 Mechanical properties of suspended graphene sheets *J. Vac. Sci. Technol.* B **25** 2558–61
[7] Lee C, Wei X D, Kysar J W and Hone J 2008 Measurement of the elastic properties and intrinsic strength of monolayer graphene *Science* **321** 385–8
[8] Liu F, Ming P M and Li J 2007 *Ab initio* calculation of ideal strength and phonon instability of graphene under tension *Phys. Rev.* B **76** 064120
[9] Jiang J W, Wang J S and Li B W 2009 Young's modulus of graphene: a molecular dynamics study *Phys. Rev.* B **80** 113405
[10] Meric I, Han M Y, Young A F, Ozyilmaz B, Kim P and Shepard K L 2008 Current saturation in zero-bandgap, topgated graphene field-effect transistors *Nature Nanotechnol.* **3** 654–9

[11] Pang S P, Tsao H N, Feng X L and Mullen K 2009 Patterned graphene electrodes from solution-processed graphite oxide films for organic field-effect transistors *Adv. Mater.* **21** 3488

[12] Cong C X, Yu T, Ni Z H, Liu L, Shen Z X and Huang W 2009 Fabrication of graphene nanodisk arrays using nanosphere lithography *J. Phys. Chem.* C **113** 6529–32

[13] Ponomarenko L A, Schedin F, Katsnelson M I, Yang R, Hill E W, Novoselov K S and Geim A K 2008 Chaotic Dirac billiard in graphene quantum dots *Science* **320** 356–8

[14] Dayen J F, Mahmood A, Golubev D S, Roch-Jeune I, Salles P and Dujardin E 2008 Side-gated transport in focused-ion-beam-fabricated multilayered graphene nanoribbons *Small* **4** 716–20

[15] Bai J W, Zhong X, Jiang S, Huang Y and Duan X F 2010 Graphene nanomesh *Nature Nanotechnol.* **5** 190–4

[16] Liang X G, Jung Y S, Wu S W, Ismach A, Olynick D L, Cabrini S and Bokor J 2010 Formation of bandgap and subbands in graphene nanomeshes with sub-10 nm ribbon width fabricated via nanoimprint lithography *Nano Lett.* **10** 2454–60

[17] Allen M J, Tung V C, Gomez L, Xu Z, Chen L M, Nelson K S, Zhou C W, Kaner R B and Yang Y 2009 Soft transfer printing of chemically converted graphene *Adv. Mater.* **21** 2098–102

[18] Wei Z Q, Barlow D E and Sheehan P E 2008 The assembly of single-layer graphene oxide and graphene using molecular templates *Nano Lett.* **8** 3141–5

[19] Fischbein M D and Drndic M 2008 Electron beam nanosculpting of suspended graphene sheets *Appl. Phys. Lett.* **93** 3

[20] Lemme M C, Bell D C, Williams J R, Stern L A, Baugher B W H, Jarillo-Herrero P and Marcus C M 2009 Etching of graphene devices with a helium ion beam *ACS Nano* **3** 2674–6

[21] Bell D C, Lemme M C, Stern L A, Rwilliams J and Marcus C M 2009 Precision cutting and patterning of graphene with helium ions *Nanotechnology* **20** 5

[22] Zhou Y and Loh K P 2010 Making patterns on graphene *Adv. Mater.* **22** 3615–20

[23] Fabbro R, Fournier J, Ballard P, Devaux D and Virmont J 1990 Physical study of laser-produced plasma in confined geometry *J. Appl. Phys.* **68** 775–84

[24] Plimpton S 1995 Fast parallel algorithms for short-range molecular-dynamics *J. Comput. Phys.* **117** 1–19

[25] Cheng G J and Shehadeh M A 2006 Multiscale dislocation dynamics analyses of laser shock peening in silicon single crystals *Int. J. Plast.* **22** 2171–94

[26] Zhao H and Aluru N R 2010 Temperature and strain-rate dependent fracture strength of graphene *J. Appl. Phys.* **108** 5

[27] Zhao H, Min K and Aluru N R 2009 Size and chirality dependent elastic properties of graphene nanoribbons under uniaxial tension *Nano Lett.* **9** 3012–5

[28] Ji J, Gao H A and Cheng G J 2010 Forming limit and fracture mode of microscale laser dynamic forming *J. Manuf. Sci. Eng.* **132** 061005

[29] Shenderova O A, Brenner D W, Omeltchenko A, Su X and Yang L H 2000 Atomistic modeling of the fracture of polycrystalline diamond *Phys. Rev.* B **61** 3877–88

[30] Grantab R, Shenoy V B and Ruoff R S 2010 Anomalous strength characteristics of tilt grain boundaries in graphene *Science* **330** 946–8